

Quantification of Lung Tumor Motion and Optimization of Treatment

Milovan Savanović (PhD Candidate)^{1,2*}, Bojan Štrbac (PhD)³, Dražan Jaroš (PhD Candidate)^{4,5}, Mauro Loi (MD)², Florence Huguet (PhD)², Jean-Noël Foulquier (PhD)²

ABSTRACT

Background: Mobility of lung tumors is induced by respiration and causes inadequate dose coverage.

Objective: This study quantified lung tumor motion, velocity, and stability for small (≤ 5 cm) and large (> 5 cm) tumors to adapt radiation therapy techniques for lung cancer patients.

Material and Methods: In this retrospective study, 70 patients with lung cancer were included that 50 and 20 patients had a small and large gross tumor volume (GTV). To quantify the tumor motion and velocity in the upper lobe (UL) and lower lobe (LL) for the central region (CR) and a peripheral region (PR), the GTV was contoured in all ten respiratory phases, using 4D-CT.

Results: The amplitude of tumor motion was greater in the LL, with motion in the superior-inferior (SI) direction compared to the UL, with an elliptical motion for small and large tumors. Tumor motion was greater in the CR, rather than in the PR, by 63% and 49% in the UL compared to 50% and 38% in the LL, for the left and right lung. The maximum tumor velocity for a small GTV was 44.1 mm/s in the LL (CR), decreased to 4 mm/s for both ULs (PR), and a large GTV ranged from 0.4 to 9.4 mm/s.

Conclusion: The tumor motion and velocity depend on the tumor localization and the greater motion was in the CR for both lobes due to heart contribution. The tumor velocity and stability can help select the best technique for motion management during radiation therapy.

Citation: Savanović M, Štrbac B, Jaroš D, Loi M, Huguet F, Foulquier JN. Quantification of Lung Tumor Motion and Optimization of Treatment. *J Biomed Phys Eng.* 2023;13(1):65-76. doi: 10.31661/jbpe.v0i0.2102-1278.

Keywords

Lung Cancer; Tumor Motion; Tumor Velocity; Tumor Stability; Four-Dimensional Computed Tomography; Stereotactic Body Radiotherapy; Radiotherapy; Intensity-Modulated Radiotherapy

Introduction

Lung cancer is a leading cause of death, common in both males and females worldwide [1]. Selecting the treatment of localized lung cancer by surgery or radiation therapy mainly depends on the stage of the tumor [2, 3]. Radiation therapy has been consistently developing to consider as an excellent solution for inoperable patients or those who are unwilling or unable to undergo surgery [4].

Lung tumors are mobile, induced by respiration (diaphragm motion and lung expansion), the heartbeat, and heart motion [5]. Tumor motion may cause inadequate dose coverage and an increased risk for local failure and/or toxicity to normal tissue [6, 7]. Although the helical CT

¹Faculty of Medicine, University of Paris-Saclay, 94276 Le Kremlin-Bicêtre, France

²Department of Radiation Oncology, Tenon Hospital, APHP, Sorbonne University, 75020 Paris, France

³MATER Private Hospital, Department of Physics, Eccles Street, Dublin 7, Ireland

⁴Center for Radiotherapy, International Medical Centers, Affidea, 78000 Banja Luka, Bosnia, and Herzegovina

⁵Faculty of Medicine, University of Banja Luka, 78000 Banja Luka, Bosnia, and Herzegovina

*Corresponding author: Milovan Savanović
Department of Radiation Oncology, Tenon Hospital, APHP, Sorbonne University, 75020 Paris, France
E-mail: milovan_savanovic@yahoo.com

Received: 8 February 2021
Accepted: 18 June 2021

scan acquired during free breathing provides instantaneous anatomical images (screenshot), it can often distort the real tumor volume and the positions of the organs at risk (OARs) [8, 9]. Using a 4D-CT scan for lung cancer patients, overall tumor motion and the anatomical localization of the OARs can be evaluated within the respiratory cycle [10, 11]. For large tumor motion, some techniques were developed based on the patient participation, the deep inspiration breath-hold (DIBH), utilization of accessories (abdominal compression), and free-breathing (respiratory gating (RGRT) or tumor tracking) to decrease tumor motion, treatment volume, and consequently sparing the OARs [12].

Free-breathing techniques result in reducing the number of patient participation and treatment performed with RGRT and tumor tracking can theoretically decrease treatment volume and spare healthy tissues more effectively [13, 14]. RGRT causes the irradiation of the tumor in certain phases of the respiratory cycle, at end-expiration or end-inspiration. The treatment volume will decrease, limiting geometrical uncertainty due to tumor motion and reducing toxicity. Tumor tracking can be performed during tumor motion through the respiratory cycle, keeping the tumor within the path of the radiation beam. With tracking, the planning target volume (PTV) and dose to the OARs can be reduced, respecting tumor velocity and the limitation of the multi-leaf collimator (MLC) velocity, uncertainties in organ motion, and set-up errors for moving tumors [15]. Selecting the motion management strategy (gating or tracking) may be influenced by tumor size, tumor localization, and tumor motion [16].

Lung tumor motion has been previously investigated in some studies where the use of different imaging techniques showed a large spread in the amplitudes of tumor motion [5]. Two studies used 4D-CT scans to evaluate three-dimensional (3D) tumor motion, depending on tumor volume and localization

on the lobe [17, 18]. Quantifying these lung tumor characteristics could reduce treatment volume and better spare healthy tissues, leading to more appropriate and personalized treatment for lung cancer patients.

The aim of this study was to quantify lung tumor motion for both small and large tumors, depending on the tumor localization, and to determine tumor velocity and stability between respiratory phases.

Material and Methods

Population

The retrospective study was conducted on a cohort of 70 consecutive patients treated between March 2017 and October 2018 in Tenon University Hospital. Out of these 70 patients, 50 patients (28 males and 22 females) with small tumors underwent Stereotactic Body Radiation Therapy (SBRT), and 20 male patients with large tumors underwent Intensity Modulated Radiation Therapy (IMRT) treatment. All of the patients included in this study were current or former tobacco smokers who were defined as more than 10 pack-years in a lifetime.

In this study, lung cancer patients received different treatment modalities according to their tumor volume. According to institutional practices, patients with small tumor sizes (≤ 5 cm) were treated with SBRT, while patients with large tumor sizes (> 5 cm) were treated with conventionally fractionated treatment using IMRT.

Data acquisition

All patients were scanned on a GE Light speed 16 slice CT (General Electric Medical Systems, Waukesha, WI), equipped with the Real-Time Positioning Management system (RPM, Varian Medical Systems, Palo Alto, CA, USA). For 4D-CT simulation, an infrared Charged-Couple Device (CCD) camera, mounted on the treatment couch, was used in conjunction with a reflective block marker

(with two reflecting dots) placed over the xiphoid process to track breathing motion during the respiratory cycle. The RPM system enables the correlation of the target's position with the patient's respiratory cycle [5].

Patients who underwent a conventionally fractionated regimen were immobilized in the supine position, with arms above their head, in the CIVCO immobilization system (CIVCO Medical Solutions, Orange City, IA, USA). Using Institutional protocol for IMRT treatment, two CT scans (with and without contrast injection) and one 4D-CT were performed.

Patients qualified for SBRT were immobilized in the supine position with arms above their head, using the BlueBAG BodyFIX immobilization system (Medical Intelligence, Schwabmünchen, Germany). The comfortable position of patients and vacuum-molded bags can reduce potential inter and intra-fraction motion [19]. Using an institutional protocol for SBRT treatment, two CT scans (with and without a stereotactic body frame) and one 4D-CT were performed.

All scans, CT and 4D-CT were performed with a 0.7 s/rotation period, 120 kV, mA ranging from 10 to 440 mA, and tube current modulation (TCM) was turned on with a field of view (FOV) of 55 cm. The only differences in the parameters were the slice thickness (1.25 mm for small and 2.5 mm for large tumors) and slice detector number (16 for small and 8 for large tumors), for the same beam collimation width (20 mm).

Delineation

To determine the amplitude of tumor motion and The Varian Eclipse 13.7 treatment planning system (TPS) is used to determine the amplitude of tumor motion and quantify its trajectory [20]. The CT scans were delineated without a stereotactic body frame (SBRT) and with injection (IMRT), for all ten phases of the respiratory cycle (eleven phases for each of the 70 patients, 770 contoured phases in total).

To compare the treatment volumes based on

the tumor motion, the internal target volume (ITV) was generated from the entire respiratory cycle versus the internal GTV (IGTV) created from stable phases only, where GTV motion can be impacted by tumor deformation or residual motion.

Data analysis

The tumor motion was analyzed and represented according to the tumor volume. The tumor trajectories were represented in statistical software Origin Pro version 8.6 (Northampton, MA, USA). The tumor motion was evaluated from the center of mass, using statistic tools from DICOM images (Digital Imaging and Communications in Medicine), calculated from the magnitude of 3D vector coordinates in each direction by equations (1, 2):

$$\|\vec{r}\| = \sqrt{x^2 + y^2 + z^2} \quad (1)$$

where x , y , and z were the left-right (LR), the anterior-posterior (AP), and the superior-inferior (SI) direction.

To calculate tumor velocity, the time necessary for the 4D-CT acquisition was also considered:

$$T = \sum_{i=1}^{10} t_i = (BC + Tr) \quad (2)$$

where BC is the breathing cycle and Tr is the tube rotation time. The time between phases was calculated using the equation (3):

$$t \geq \frac{T}{10} = \frac{(BC + Tr)}{10} \quad (3)$$

From the third equation (3), the tumor velocity is computed based on equation (4):

$$v_i = \frac{s_i}{t_i} \quad (4)$$

where s_i represents the distance and t_i the time between adjacent phases. The lung tumor motion, velocity, and stability were quantified based on the tumor's localization in the region (central region (CR) ≤ 2 cm from mediastinum or peripheral region (PR) > 2 cm from mediastinum), lobe (upper or lower), and lung (left

or right).

Median values were compared using a multivariable test (significance level: $P < 0.05$) and statistical analysis was done using the statistical software SEM (SILEX Development, Mirefleurs, France).

Results

Patients' characteristics

The characteristics of the patients are presented in Table 1. Among the patients included in this study, 61.5% had a tumor located in the UL, and 38.5% in the LL. 58% and 42% of patients with small tumors, the tumor was located in the UL and the LL, respectively; while for 65% and 35% of patients with large tumors, the tumor was located in the UL and the LL.

Tumor motion

The motion and trajectory of tumors are presented below, depending on tumor localization in the lung.

Figure 1 shows the tumor motion in the UL

Table 1: Patient characteristics.

Patient characteristics		
Age (years old)	Median	67
	Range	38-90
Sex (n; %)	Male	48 (68.5)
	Female	22 (31.5)
Tumor localization (n; %)	Right lung	38 (54)
	Upper lobe	26 (68)
	Lower lobe	12 (32)
	Left lung	32 (46)
	Upper lobe	15 (47)
Tumor size (n; %)	≤ 5 cm	50 (71.5)
	> 5 cm	20 (28.5)
	Treatment technique (n; %)	
	SBRT	50 (71.5)
	IMRT	20 (28.5)

SBRT: Stereotactic body radiation therapy, IMRT: Intensity modulated radiation therapy

can be complex. For small tumors, the tumor's motion with its trajectory was presented in different forms of tumor motion, where 94% of the motion was elliptical (presented for six patients), 4% was diagonal (two patients) and 2% was anterior-posterior (one patient).

For small tumors, Figure 2 reveals the tumor motion in the LL, performed in the SI direction for five patients with (44%) and without hysteresis (56%), for both regions, CR and PR.

The results of the tumor motion were presented in the UL and LL, depending on the lung (left vs. right) and region of the tumor's localization (CR vs. PR), for small tumors and also depending on the lung (left vs. right), for large tumors (Table 2).

The tumor motion was greater in the CR rather than in the PR, by 63% in the UL and 50% in the LL for the right lung, and by 49% in the UL and 38% in the LL for the left lung. A greater amplitude of tumor motion was in

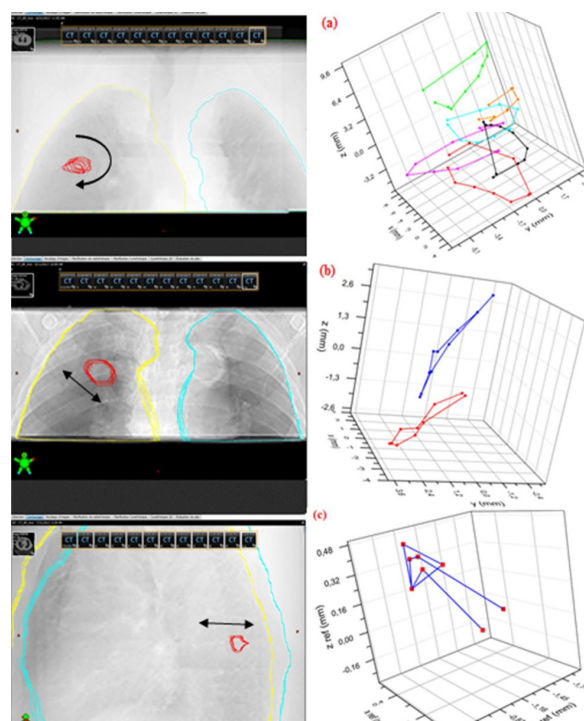


Figure 1: Tumor motion through all ten phases with tumor trajectory in the upper lobe for small tumors presented elliptical motion (a), diagonal motion (b) and motion in the antero-posterior (AP) direction (c).

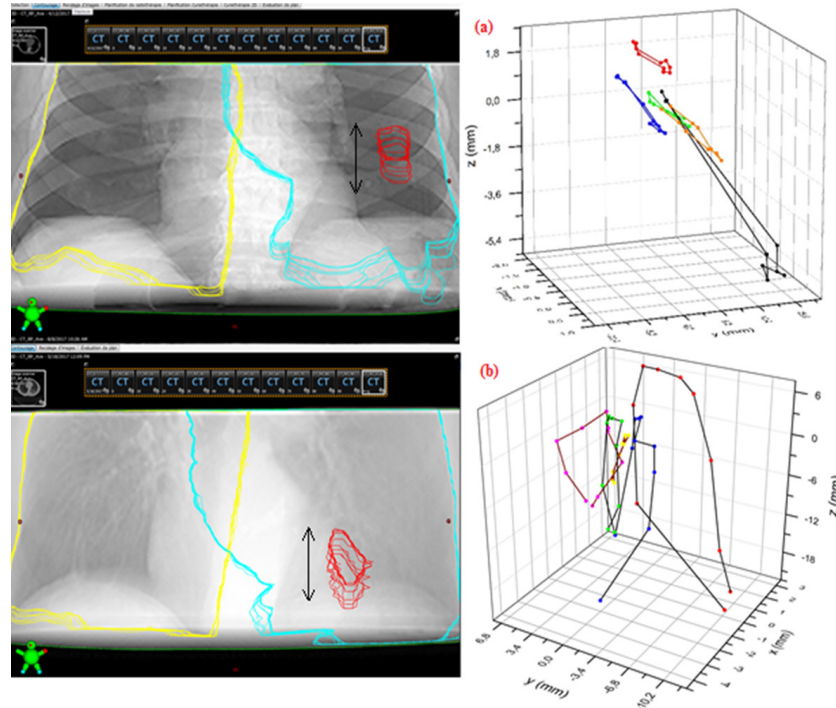


Figure 2: The tumor motion and trajectory of tumor motion presented for five patients in the superior-inferior direction without hysteresis (a) and for five patients in the superior-inferior direction with hysteresis (b), in the lower lobe, for small tumors.

the LL (ranged from 2.1 to 3.5 times) rather than in the UL, for both small and large tumors.

In multivariable analysis, small tumors moved differently between the CR and PR in the x-direction ($P < 0.0001$) and y-direction ($P < 0.0001$). The difference in the z-direction was significant when comparing the left versus the right lung $P = 0.001$, the UL versus the LL $P = 0.0001$, and small versus large tumors $P = 0.036$. The factor related to $\|\vec{r}\|$ was significantly different between central versus peripheral tumors $P < 0.0001$, the left versus the right lung $P = 0.003$, the UL versus the LL $P < 0.0001$, and small versus large tumors $P = 0.031$.

The overall tumor motion $\|\vec{r}\|$ and tumor volume for small tumors is shown for the UL and LL depending on the region of the tumor's localization (CR versus PR) (Figure 3).

Based on this, the limit of the overall tumor motion is distinguished between the CR and PR in the UL (3 mm) and LL (10 mm). For

the UL, the median and maximum overall motion were 2 mm and 3 mm, respectively, in the PR and were also 6 mm and 10 mm in the CR respectively. In the LL, the median and the maximum overall motion were 6 mm and 9.2 mm in the PR, respectively, and 15 mm and 24 mm in the CR respectively.

Heart contribution in tumor motion was presented with the distance between heart and tumor, in the UL and LL (Figure 4).

Tumor velocity

Table 3 shows the tumor's velocity that for small tumors was evaluated depending on the lobe (UL versus LL), lung (left versus right), and region (CR versus PR). The velocity for large tumors was evaluated depending on the lobe (UL versus LL) and lung (left versus right).

Tumor velocity was significantly different when comparing the left versus the right lung $P = 0.006$, the UL versus the LL ($P < 0.0001$), and small versus large tumors $P = 0.031$, using

Table 2: Tumor motion (in all directions with a radius vector) and tumor volume presented with median values and ranges, for both small and large tumors, in the upper and lower lobes, depending on the region of the tumor’s localization (central versus peripheral).

Lobe	Small tumors				Large tumors	
	Central		Peripheral		Left	Right
	Left	Right	Left	Right		
Upper lobe						
x (mm)	2.3 (0.5-7.5)	2.9 (0.6-4.4)	0.7 (0.5-1.1)	0.7 (0.5-1.5)	2.3 (0.9-2.6)	1.1 (0.1-3.3)
y (mm)	2.7 (1.8-4.2)	3.8 (1.6-9.8)	1.6 (0.6-2.4)	1.2 (0.3-2.3)	1.4 (0.7-2.4)	1.8 (0.2-3.6)
z (mm)	3.1 (1.5-5.4)	2.8 (0.1-3.7)	1.2 (1.1-1.3)	1.3 (0.4-2.8)	0.4 (0.3-2.4)	1.4 (0.2-3.5)
$\ \vec{r}\ $ (mm)	4.3 (3.2-10.0)	5.4 (3.5-10.1)	2.2 (1.2-2.5)	2.0 (0.6-2.8)	2.7 (1.2-3.6)	2.5 (0.2-4.8)
Volume (cc)	3.6 (0.9-8.1)	3.7 (0.7-8.6)	2.3 (0.7-9.3)	2.4 (0.4-16.5)	96.8 (41.5-119.7)	94.3 (11.2-479.3)
Lower lobe						
x (mm)	2.1 (1.2-3.0)	2.5 (1.2-3.8)	0.8 (0.4-2.2)	1.0 (0.6-1.3)	1.7 (0.7-2.6)	1.0 (0.5-2.0)
y (mm)	2.1 (0.8-10.3)	3.8 (2.5-5.0)	1.8 (0.5-2.7)	1.0 (0.9-1.2)	2.1 (1.8-2.4)	1.2 (0.7-2.9)
z (mm)	12.3 (10.7-21.7)	10.8 (5.6-15.9)	6.5 (0.4-8.9)	6.5 (3.8-8.7)	6.5 (6.2-6.7)	4.5 (1.5-6.5)
$\ \vec{r}\ $ (mm)	12.5 (10.9-24.0)	11.3 (10.0-16.6)	7.7 (1.9-9.2)	6.6 (4.0-8.6)	7.0 (6.4-7.3)	4.8 (2.5-6.5)
Volume (cc)	3.4 (1.3-6.2)	1.2 (0.5-1.8)	1.6 (0.6-9.3)	5.0 (3.5-11.9)	298.6 (14.6-582.6)	98.2 (44.4-194.0)

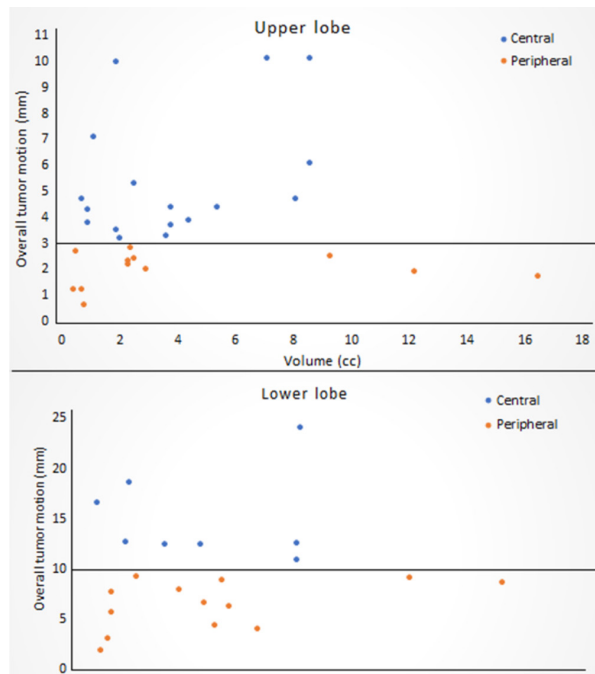


Figure 3: The overall tumor motion $\|\vec{r}\|$ and tumor volume presented in the upper lobe (up) and lower lobe (down), depending on the region of the tumor’s localization (central versus peripheral), for small tumors.

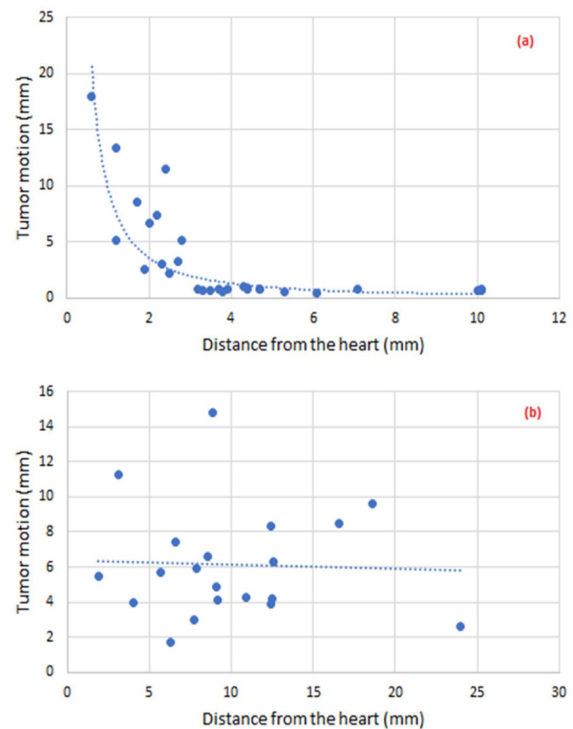


Figure 4: Decrease in tumor motion with distance from the heart in the upper lobe (a) and lower lobe (b) for small tumors.

Table 3: Results of the tumor's velocity for small and large tumors, depending on the lobe and region.

Lobe	SBRT				IMRT	
	Central		Peripheral		Large tumor	
	Left	Right	Left	Right	Left	Right
UL (mm/s)	6.8 (1.2-11.0)	4.3 (0.9-10.0)	1.4 (0.3-3.6)	3.1 (0.3-4.3)	1.4 (0.4-3.6)	3.3 (0.4-6.7)
LL (mm/s)	18.5 (1.8-44.1)	3.4 (1.7-20.2)	9.1 (0.7-15.0)	6.0 (0.4-10.9)	3.2 (0.4-6.3)	4.9 (0.6-9.4)

SBRT: Stereotactic body radiation therapy, IMRT: Intensity modulated radiation therapy, UL: Upper lobe, LL: lower lobe

multivariable analysis.

The tumor's velocity depends on the phases through the respiratory cycle for each phase and three different cases as seen in Figure 5.

The tumor's velocity varies and depends on phases that in some phases, the tumor velocity is constant (30-60% phases, 30-70% phases, and 40-70% phases) with a small residual tumor motion, named "tumor stability". The velocity between stable phases varies from 0.3 to 4.1 mm/s. This residual motion was less than 3 mm between stable phases.

Tumor stability

For both small and large tumors, the characteristics of tumor stability in the UL and LL are represented in Table 4. The difference in the volumes was represented using the ITV for the entire respiratory cycle and the IGTV for stable phases.

Comparing the ITV versus IGTV volumes, significant results were $P < 0.001$, UL versus LL ($P < 0.0001$), and small versus large tumors $P < 0.0001$.

Discussion

In this study, tumor motion was evaluated in different localizations depending on the regions (CR versus PR), lungs' side (left versus right), and lobes (UL versus LL), in all directions, based on the overall tumor motion. The amplitude of overall tumor motion decreased by a factor of about 2 in the PR compared to the CR, for both lungs and lobes. In the UL, larger tumor motion was in all directions in the

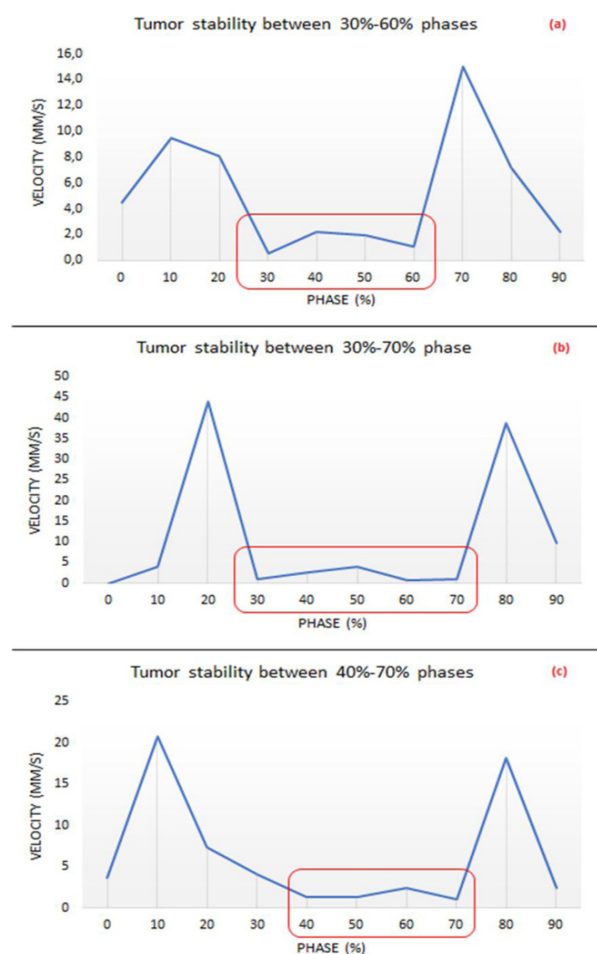


Figure 5: Tumor velocity with tumor stability between 30-60% phase, in the peripheral region for left lower lobe (a), the highest tumor velocity and tumor stability between 30-70% phases in the central region for the left lower lobe (b), and tumor velocity with tumor stability between 40-70% phases, in the central region for the right lower lobe (c).

Table 4: Comparison of the internal target volume (ITV) volume from total motion and internal gross tumor volume (IGTV) volume from stable phases, for small and large tumors, depending on tumor localization on the lobe (upper versus lower).

Volume	Lobe	Patient (%)	Phase (%)	ITV (cc)	IGTV (cc)	(ITV-IGTV)/ITVx100 (%)
Small tumor	UL	52	30 – 60	4.3	2.1	51
		25	30 – 70	2.1	1.5	29
		23	40 – 70	11.2	7.9	29
	LL	33	30 – 60	14.6	2.5	83
		22	30 – 70	1.8	0.9	50
		45	40 – 70	11.6	6.4	49
Large tumor	UL	80	30 – 60	248.5	82.8	67
		20	30 – 70	317.1	99.1	69
	LL	43	30 – 60	195.1	45.6	77
		57	30 – 70	59.0	19.4	67

ITV: Internal target volume, IGTV: Nternal gross tumor volume, UL: Upper lobe, LL: Lower lobe

CR rather than in the PR, i.e. 4.3 times in the x-direction, 3.2 times in the y-direction, and 2.6 times in the z-direction. In the LL, these factors decreased in the x-direction (2.5 times) and z-direction (1.9 times), with the same factor value (3.2 times) in the y-direction, comparing the CR versus the PR. Based on some studies, the amplitude of tumor motion depends on the localization of tumors, increasing when the tumor approaches the diaphragm, especially in the SI direction [17, 21-23]. In this study, the median values of tumor motion were greater than in previously cited studies.

For small tumors, heart contribution was more pronounced in the CR rather than in the PR, by 2.7 times in the UL and 1.7 times in the LL for the right lung, and by 2 times in the UL and 1.6 times in the LL for the left lung. These results (Table 2) confirm that heart contribution depends on the distance from the heart and not the lungs' side (left versus right) and the amplitude of tumor motion decreases with increasing the distance from the heart.

Large tumors move with similar amplitudes to small tumors located in the PR, performing elliptical motion in the UL and SI motion in the LL that larger tumor motion was in the LL

rather than in the UL, by 62% in the left lung and 48% in the right lung.

By observing the trajectories of tumor motion, lung tumors have an elliptical motion, regardless of the lobe or region. The amplitude, orientation, and shape of the tumor motion depend on the localization of the tumor in the lungs due to different contributions of the heartbeat and heart motion, diaphragm motion, and lung expansion. Elliptical motion can be presented using the equation (5):

$$\frac{x^2}{h^2} + \frac{y^2}{l^2} + \frac{z^2}{d^2} = 1 \tag{5}$$

where x , y , and z are coordinates and h represents heartbeat contribution during motion. Also, l and d represent lung expansion during respiration and the contribution of the diaphragm motion.

The heart contribution was more pronounced in the UL, especially in the CR that the heartbeat and heart motion creates a complex tumor motion (Figure 1). Tumors located in the UL of either the left or right lung, moved with an amplitude larger than 10 mm in 38% of elliptical motion (a), due to contribution by all of the parameters from the equation (5). The amplitude and orientation of the elliptical mo-

tion depend on tumor localization and distance from the heart, represented with a range of motion in the x (from 0.5 mm to 7.5 mm) and y (from 1.8 to 4.2 mm) directions in the left lung, and x (from 0.6 mm to 4.4 mm) and y (from 1.6 to 9.8 mm) directions in the right lung (Table 2).

However, in the second case, tumors located in the lower part of the UL moved in a diagonal direction (b), a direct consequence of the resultant forces of the diaphragm's and heart movements (without significant lung expansion in the y -direction), where $h = d \gg l$ (equation (6)).

$$\frac{x^2}{h^2} + \frac{z^2}{d^2} = 1 \quad (6)$$

In the third case, small tumors located in the UL near the upper portion of the heart, consequently, move in the antero-posterior direction by lung expansion (c), i.e. $h = d < l$ due to the equal forces between the heartbeat and diaphragm motions (equation (7)).

$$\frac{x^2}{h^2} + \frac{y^2}{l^2} = 1 \quad (7)$$

According to the motions in the UL, the trajectory of tumor motion was quasi symmetrical in all directions (x , y , and z), extending the PTV with a uniform margin.

For tumors located in the LL, the predominant direction of motion was the SI, due to diaphragm motion, i.e. $d \gg h, l$ (without significant lung expansion in the y -direction), regardless of tumor size (equation (8)).

$$\frac{y^2}{l^2} + \frac{z^2}{d^2} = 1 \quad (8)$$

In the CR, the motion in the SI direction was impacted by the heartbeat and heart motion and tumors moved with hysteresis (b), i.e. $h, l < d$ for $h, l \neq 0$ (equation (6)).

Motion with hysteresis increases the amplitude of tumor motion, increasing the treatment volume and geographic misses during treatment [23]. Due to tumor motion in the SI di-

rection, the PTV margin will extend in the vertical direction, for tumors located in the LL.

In the current study, greater velocity was in the LL rather than in the UL after analyzing the results of tumor velocity for both (small and large) tumors with greater tumor velocity in the CR, especially in the left lung. In some cases, tumor velocity could predetermine the treatment technique. If the tumor velocity was not constant and very fast >25 mm/s, the treatment solution is based on ITV according to overall tumor motion through all ten phases. The results of this study show that tumor velocity changed during the respiratory cycle and depended on the phase. In some phases, the tumor velocity could be greater than the velocity of an MLC, and also, in turn, introduce additional geometric uncertainty during treatment delivery. In this study, 10% of the patients had tumor velocity greater than the MLC velocity (25 mm/s, TrueBeam Novalis STx, in our institution), with tumors located in the left lower lobe, in the CR. In the Shirato et al. study, 29% of patients had a maximum velocity of 33 mm/s, evaluating the tumor velocity from the velocity of fiducial markers [24]. The tumor tracking can be used only with an MLC velocity superior to 45 mm/s.

In the case of constant and smaller velocity (<5 mm/s), stable phases can be determined between several phases, where velocity decreases and acceleration is also reduced to zero. For 98% and 2% of our patients with small tumors, tumor stability was at end-expiration and end-inspiration, respectively.

With 85% of our patients, tumor stability was during 4 phases. In the right lung (23 patients – 46%), tumors were more stable in the UL (70% of tumors) rather than in the LL (30% of tumors). Whereas, tumors located in the left lung (27 patients – 54%) were more stable in the LL (56% of tumors) rather than in the UL (44% of tumors). In the UL, stability was between 30% to 60% phases, shifting to 40% to 70% phases, depending on the tumor localization (oblique fissure – limit between

the UL and LL). Generally, tumors located in the upper portion of the LL are stable between 30–60%. In the lower part of the LL, the stability of phases decreased from 30-70% to 40–70% with irregular patient respiration. Lee et al. generally used a duty cycle of 40%-60% phases, shifting to 30%-70% phases for regular and stable respiration [25].

Variations in the stable phases came from tumor deformation, changing volumes and the isocenter of the GTV in DICOM images, creating a small shift between phases (residual motion) that occurs between stable phases from residual motion (less than 3 mm), i.e. decreasing the residual motion between stable phases, decreasing velocity. The RGRT technique would be the best solution using a gating window on stable phases. Regarding the residual motion on stable phases, the margin inside the gating window can be calculated from the tumor velocity:

$$\Delta x = \frac{T \times \Delta n}{10} \times v_{min} \tag{9}$$

where Δx is the calculated margin, T is the time of the breathing cycle, Δn – the number of the stable phases and v_{min} – the minimum tumor velocity.

Figure 6 shows velocity and localization, depending on patient respiration (regular vs irregular) and the organizational chart of the treatment in the lung cancer tumors.

According to the American Association of Physics in Medicine (AAPM) task group 76

report, the RGRT technique can be employed when tumor motion exceeds 5 mm [5]. In this study, only 22% of tumors moved more than 10 mm, while 32% of tumors moved more than 5 mm, for patients with small tumors, whereas 20% of the patients with large tumors had tumor motion greater than 5 mm. Liu et al. found that 39.2% of tumors move more than 5 mm and 10.8% of tumors move more than 10 mm [18]. Sarudis et al. reported that tumor motion ≥ 1 cm was in 46.3% of tumors located in the LL and 6.7% of the tumors in the UL [17].

Using the RGRT technique on 4 or 5 stable phases, the significant difference ($P < 0.001$) was compared to the volume from the stable phases (IGTV) to the volume from the entire respiratory cycle (ITV). The better result was in the LL due to a larger ITV, provided from a larger amplitude of tumor motion. An important reduction in treatment volume was for both small and large tumors, using treatment based on the stable phases (Table 4), decreasing treatment volume. In the Underberg et al. study, the PTV volume gain obtained between the PTV volume from an entire respiratory cycle and the PTV volume from stable phases was more than 30% in 38% of tumors and more than 50% in 15% of tumors [26].

The current study has some limitations, such as a small patient’s cohort, manual contouring of tumor volumes, and retrospective calculation of the tumor motion and velocity and

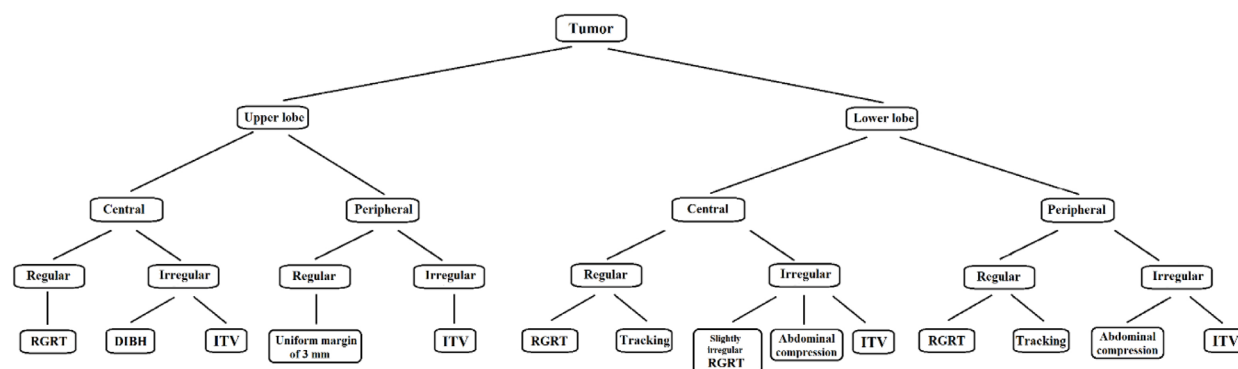


Figure 6: Organizational chart of lung cancer treatment depending on tumor motion, tumor localization in the lung (upper lobe and lower lobe) and region (central vs peripheral), and patient respiration.

some comparisons were limited due to geometrical and volumetric differences between the lungs and lobes.

Conclusion

In this study, the quantification of lung tumor motion and optimization of their treatment were investigated. Tumor motion was predominant elliptical in the UL and the SI direction in the LL and greater tumor motion was in the CR, for both lobes and lungs with differences in motion between the tumors located in the CR and PR, for both lungs from heart contribution, while the amplitude of tumor motion depends on the distance from the heart. The results of tumor motion can be used to predict the ITV and determine the shape and direction of the PTV margin. Due to the different shapes of tumor motion, we can expect PTV expansion in the vertical direction for the LL and a uniform expansion in the UL.

The selection of treatment can be based on tumor stability and tumor velocity, influenced by the tumor's localization and the phase of the respiratory cycle. When the velocity decreases in a certain phase, the tumor becomes stable due to a constant velocity, allowing for an important reduction in the treatment volume, which can decrease the dose received by the surrounding healthy tissues, using the RGRT technique. For tumors that do not have stable phases, the treatment of choice could be tumor tracking, if tumor velocity does not exceed the MLC velocity.

Authors' Contribution

M. Savanovic conceived the idea. Introduction of the paper was written by M. Savanovic, B. Strbac, D. Jaros and F. Huguet gather the images and the related literature and also help with writing of the related works. The method implementation was carried out by M. Savanovic, B. Strbac, D. Jaros and JN. Foulquier. Results and Analysis was carried out by M. Savanovic, M. Loi, F. Huguet and JN. Foulquier. The research work was proof-read and supervised by M. Savanovic, M. Loi, F. Huguet and JN. Foulquier. All the authors read,

modified, and approved the final version of the manuscript.

Ethical Approval

Ethical approval was waived by the local Ethics Committee of University Paris VI in view of the retrospective nature of the study and all the procedures being performed were part of the routine care.

Informed Consent

The authors affirm that human research participants provided informed consent for publication.

Conflict of Interest

None

References

1. Didkowska J, Wojciechowska U, Mańczuk M, obaszewski J. Lung cancer epidemiology: contemporary and future challenges worldwide. *Ann Transl Med.* 2016;**4**(8):150. doi: 10.21037/atm.2016.03.11. PubMed PMID: 27195268. PubMed PMCID: PMC4860480.
2. Lemjabbar-Alaoui H, Hassan OU, Yang YW, Buchanan P. Lung cancer: Biology and treatment options. *Biochim Biophys Acta.* 2015;**1856**(2):189-210. doi: 10.1016/j.bbcan.2015.08.002. PubMed PMID: 26297204. PubMed PMCID: PMC4663145.
3. Travis WD, Brambilla E, Riely GJ. New pathologic classification of lung cancer: relevance for clinical practice and clinical trials. *J Clin Oncol.* 2013;**31**(8):992-1001. doi: 10.1200/JCO.2012.46.9270. PubMed PMID: 23401443.
4. Fernandez C, Grills IS, Ye H, Hope AJ, et al. Stereotactic Image Guided Lung Radiation Therapy for Clinical Early Stage Non-Small Cell Lung Cancer: A Long-Term Report From a Multi-Institutional Database of Patients Treated With or Without a Pathologic Diagnosis. *Pract Radiat Oncol.* 2020;**10**(4):e227-37. doi: 10.1016/j.prro.2019.12.003. PubMed PMID: 31837478.
5. Keall PJ, Mageras GS, Balter JM, et al. The management of respiratory motion in radiation oncology report of AAPM Task Group 76. *Med Phys.* 2006;**33**(10):3874-900. doi: 10.1118/1.2349696. PubMed PMID: 17089851.
6. Liauw SL, Connell PP, Weichselbaum RR. New paradigms and future challenges in radiation oncology: an update of biological targets and technology. *Sci Transl Med.* 2013;**5**(173):173sr2. doi: 10.1126/scitranslmed.3005148. PubMed PMID: 23427246. PubMed PMCID: PMC3769139.
7. Chi A, Nguyen NP, Welsh JS, Tse W, et al. Strategies of dose escalation in the treatment of locally ad-

- vanced non-small cell lung cancer: image guidance and beyond. *Front Oncol.* 2014;**4**:156. doi: 10.3389/fonc.2014.00156. PubMed PMID: 24999451. PubMed PMCID: PMC4064255.
8. Fukui M, Takamochi K, Matsunaga T, et al. Risk of the preoperative underestimation of tumour size of lung cancer in patients with idiopathic interstitial pneumonias. *Eur J Cardiothorac Surg.* 2016;**50**(3):428-32. doi: 10.1093/ejcts/ezw065. PubMed PMID: 26987880.
 9. Lampen-Sachar K, Zhao B, Zheng J, et al. Correlation between tumor measurement on Computed Tomography and resected specimen size in lung adenocarcinomas. *Lung Cancer.* 2012;**75**(3):332-5. doi: 10.1016/j.lungcan.2011.08.001. PubMed PMID: 21890229. PubMed PMCID: PMC4441034.
 10. Bai T, Zhu J, Yin Y, Lu J, Shu H, Wang L, Yang B. How does four-dimensional computed tomography spare normal tissues in non-small cell lung cancer radiotherapy by defining internal target volume? *Thorac Cancer.* 2014;**5**(6):537-42. doi: 10.1111/1759-7714.12126. PubMed PMID: 26767049. PubMed PMCID: PMC4704343.
 11. Aznar MC, Persson GF, Kofoed IM, Nygaard DE, Korreman SS. Irregular breathing during 4DCT scanning of lung cancer patients: is the midventilation approach robust? *Phys Med.* 2014;**30**(1):69-75. doi: 10.1016/j.ejmp.2013.03.003. PubMed PMID: 23590980.
 12. Qian J, Xing L, Liu W, Luxton G. Dose verification for respiratory-gated volumetric modulated arc therapy. *Phys Med Biol.* 2011;**56**(15):4827-38. doi: 10.1088/0031-9155/56/15/013. PubMed PMID: 21753232. PubMed PMCID: PMC3360016.
 13. Giraud P, Morvan E, Claude L, Mornex F, Le Pechoux C, et al. Respiratory gating techniques for optimization of lung cancer radiotherapy. *J Thorac Oncol.* 2011;**6**(12):2058-68. doi: 10.1097/JTO.0b013e3182307ec2. PubMed PMID: 22052228.
 14. Prunareddy J, Boisselier P, Aillères N, Riou O, Simeon S, Bedos L, Azria D, Fenoglietto P. Tracking, gating, free-breathing, which technique to use for lung stereotactic treatments? A dosimetric comparison. *Rep Pract Oncol Radiother.* 2019;**24**(1):97-104. doi: 10.1016/j.rpor.2018.11.003. PubMed PMID: 30532657. PubMed PMCID: PMC6261085.
 15. Cozzi L, Fogliata A, Thompson S, Franzese C, et al. Critical Appraisal of the Treatment Planning Performance of Volumetric Modulated Arc Therapy by Means of a Dual Layer Stacked Multileaf Collimator for Head and Neck, Breast, and Prostate. *Technol Cancer Res Treat.* 2018;**17**:1-11. doi: 10.1177/1533033818803882. PubMed PMID: 30295172. PubMed PMCID: PMC6176542.
 16. Korreman SS. Image-guided radiotherapy and motion management in lung cancer. *Br J Radiol.* 2015;**88**(1051):20150100. doi: 10.1259/bjr.20150100. PubMed PMID: 25955231. PubMed PMCID: PMC4628536.
 17. Sarudis S, Karlsson Hauer A, Nyman J, Bäck A. Systematic evaluation of lung tumor motion using four-dimensional computed tomography. *Acta Oncol.* 2017;**56**(4):525-30. doi: 10.1080/0284186X.2016.1274049. PubMed PMID: 28075183.
 18. Liu HH, Balter P, Tutt T, et al. Assessing respiration-induced tumor motion and internal target volume using four-dimensional computed tomography for radiotherapy of lung cancer. *Int J Radiat Oncol Biol Phys.* 2007;**68**(2):531-40. doi: 10.1016/j.ijrobp.2006.12.066. PubMed PMID: 17398035.
 19. Hubie C, Shaw M, Bydder S, et al. A randomised comparison of three different immobilisation devices for thoracic and abdominal cancers. *J Med Radiat Sci.* 2017;**64**(2):90-6. doi: 10.1002/jmrs.202. PubMed PMID: 27998039. PubMed PMCID: PMC5454323.
 20. Shine NS, Paramu R, Gopinath M, Jaon Bos RC, Jayadevan PM. Out-of-Field Dose Calculation by a Commercial Treatment Planning System and Comparison by Monte Carlo Simulation for Varian TrueBeam®. *J Med Phys.* 2019;**44**(3):156-75. doi: 10.4103/jmp.JMP_82_18. PubMed PMID: 31576064. PubMed PMCID: PMC6764172.
 21. Van Sörnsen De Koste JR, Lagerwaard FJ, Nijssen-Visser MR, et al. Tumor location cannot predict the mobility of lung tumors: a 3D analysis of data generated from multiple CT scans. *Int J Radiat Oncol Biol Phys.* 2003;**56**(2):348-54. doi: 10.1016/s0360-3016(02)04467-x. PubMed PMID: 12738308.
 22. Miura H, Masai N, Oh RJ, Shiomi H, Sasaki J, Inoue T. Approach to dose definition to the gross tumor volume for lung cancer with respiratory tumor motion. *J Radiat Res.* 2013;**54**(1):140-5. doi: 10.1093/jrr/rrs054. PubMed PMID: 22951318. PubMed PMCID: PMC3534263.
 23. Seppenwoolde Y, Shirato H, Kitamura K, et al. Precise and real-time measurement of 3D tumor motion in lung due to breathing and heartbeat, measured during radiotherapy. *Int J Radiat Oncol Biol Phys.* 2002;**53**(4):822-34. doi: 10.1016/s0360-3016(02)02803-1. PubMed PMID: 12095547.
 24. Shirato H, Suzuki K, Sharp GC et al. Speed and amplitude of lung tumor motion precisely detected in four-dimensional setup and in real-time tumor-tracking radiotherapy. *Int J Radiat Oncol Biol Phys.* 2006;**64**(4):1229-36. doi: 10.1016/j.ijrobp.2005.11.016. PubMed PMID: 16504762.
 25. Lee SY, Lim S, Ma SY, Yu J. Gross tumor volume dependency on phase sorting methods of four-dimensional computed tomography images for lung cancer. *Radiat Oncol J.* 2017;**35**(3):274-80. doi: 10.3857/roj.2017.00444. PubMed PMID: 29037025. PubMed PMCID: PMC5647759.
 26. Underberg RW, Lagerwaard FJ, Slotman BJ, et al. Benefit of respiration-gated stereotactic radiotherapy for stage I lung cancer: an analysis of 4DCT datasets. *Int J Radiat Oncol Biol Phys.* 2005;**62**(2):554-60. doi: 10.1016/j.ijrobp.2005.01.032. PubMed PMID: 15890600.